Interactions of self-localized optical wavepackets in reorientational soft matter

Citation for published version:
Assanto, G, Marchant, T & Smyth, NF 2022, 'Interactions of self-localized optical wavepackets in reorientational soft matter', *Applied Sciences*, vol. 12, no. 5, 2607. https://doi.org/10.3390/app12052607

Digital Object Identifier (DOI):
10.3390/app12052607

Link:
Link to publication record in Edinburgh Research Explorer

Document Version:
Peer reviewed version

Published In:
Applied Sciences

Article

Interactions of self-localized optical wavepackets in reorientational soft matter

Gaetano Assanto [1,†] *, Timothy R. Marchant [2,3†], Noel F. Smyth [3,4†]

[1] NooEL— Nonlinear Optics & OptoElectronics Lab, University of Rome "Roma Tre", 00146 Rome, Italy; gaetano.assanto@uniroma3.it
[2] Australian Mathematical Sciences Institute, University of Melbourne, Melbourne, Victoria, Australia, 3052; t.marchant@uow.edu.au
[3] School of Mathematics and Applied Statistics, University of Wollongong, Wollongong, New South Wales, Australia, 2522
[4] School of Mathematics, University of Edinburgh, Edinburgh, Scotland, EH9 3FD, U.K.; N.Smyth@ed.ac.uk
† All authors contributed equally to this work.

Abstract: The interaction of optical solitary waves in nematic liquid crystals, nematicons and vortices, with other nematicons and localised structures, such as refractive index changes, is reviewed. Such interactions are shown to enable simple routing schemes as a basis for all-optical guided wave signal manipulation.

Keywords: nematic liquid crystals; nematicon; soliton; modulation theory

Citation: Assanto, G.; Marchant, T.R.; Smyth, N.F. Interactions of self-localized optical wavepackets in reorientational soft matter. *Appl. Sci.* **2022**, *1*, 0. https://doi.org/

Received:
Accepted:
Published:

1. Introduction

The solitary wave is a ubiquitous nonlinear dispersive wave form, originally arising in water waves [1–3], but subsequently found to exist in a wide range of areas, including nonlinear optics [4–8], plasma physics [9] and biology [10,11]. A solitary wave is an isolated, most often hump-shaped wavepacket, which generally emerges as the infinite wavelength limit of a (nonlinear) periodic wave solution [2]. A special case of a solitary wave is a soliton, which is a solitary wave solution of a nonlinear dispersive wave equation which is integrable in a Hamiltonian sense through the method of inverse scattering [2,3]. Solitons exhibit "clean" interactions in that N of them interact with no change of shape or velocity, other than a phase shift. Conversely, solitary waves, in general, do not show "clean" interactions, with dispersive radiation generated upon collisions. The compact, hump-shaped form of solitary waves allow them to be modelled as particles, especially in their collisions and particularly for the integrable case of solitons for which no radiation is generated on interaction [12].

Solitary waves stem from a balance between self-phase modulation (self-focusing) and dispersion (diffraction). As such, they can be generated in nonlinear optical media, such as optical fibres [4,6] and soft matter [7,13], for which nonlinear self-effects owing to an intensity dependent refractive index or self-phase modulation balances diffraction or dispersion. Nematic liquid crystals (NLC), a family of organic soft matter encompassing optical birefringence and positive uniaxiality in a fluid state with a large degree of orientational order, are an ideal medium in which to excite solitary waves due to the "huge" nonlinear response to optical forcing, many orders of magnitude larger than, e.g., in glass fibres [7,13,14]. This results in all-optical effects which can be observed at mW powers over millimetre distances [14], rather than the kilometers typical of communication fibres [4]. Since their indisputable demonstration in 2000 [14] there have been extensive studies, both experimental and theoretical/numerical, of nematicons (i.e., solitary waves in NLC) and other optical solitary-type waves in NLC, such as optical vortices, see [7,8,15–19] for reviews of this work. The present paper is a synopsis on the interaction of nematicons and optical vortices with each other and with regions of refractive index variations in NLC samples. The motivation behind such studies is the all-optical control of optical solitary wave trajectories towards applications, such as signal processing and all-optical waveguiding/routing [20–30]. Before describing specific cases of solitary wave interactions in planar NLC samples, the equations governing nonlinear optical wavepacket propagation will be summarised to set the examples in context.

One of the main difficulties in the theoretical modelling of nematicon propagation and dynamics is the lack of any exact general solitary waves solutions of the NLC equations. The only exact solutions which exist are isolated ones for fixed parameter values [31], not suitable for modelling the general evolution of light beams in nematic liquid crystals. While the NLC equations can be solved using computational methods, analytical solutions give insights into the dynamics which are not available from numerical solutions. One powerful analytical tool is modulation theory [2], originally based on assuming a slowly varying wavetrain that is an exact solution of the underlying nonlinear dispersive wave equation, but with slowly evolving parameters. The basic assumption is that the wavetrain evolves on a slower scale than its wavelength; for slowly varying solitary waves, modulation theory (MT) essentially treats them as particles in a potential [12]. To extend MT to nonlinear dispersive wave equations without exact general solitary wave solutions, variational methods have proved to be useful, see [32] for an overview of these. The idea is that the unknown beam profile in approximated by some functional form, often a Gaussian in the case of light beams as the input laser beam has a Gaussian profile. The MT equations describing the evolution of a slowly varying beam can then be derived either from a Lagrangian formulation of the governing equations or from conservation equations [32]. In this Paper theoretical results derived using this extension of MT will be presented with pertinent experimental and numerical results, where appropriate.

2. NLC Equations

Let us consider the propagation of a linearly, extraordinarily polarized, coherent light beam of wavenumber k_0, wavelength $\lambda_0 = 2\pi/k_0$, through a planar cell filled with fully oriented nematic liquid crystals. The beam is assumed to propagate down the cell in the Z direction, with its electric field E initially oscillating in the Y direction. The coordinate X then completes the coordinate triad. The refractive indices of the medium are $n_\parallel$ for light polarized along the molecular director $\hat{\mathbf{n}}$ (long axis of the molecules) and $n_\perp$ for fields polarized orthogonal to it. The molecular director $\hat{\mathbf{n}}$ corresponds to the optic axis of the positive uniaxial medium with $n_\parallel > n_\perp$. A fundamental property of oriented NLC is the Freédericksz transition, whereby a threshold optical power (or electric voltage) is needed to rotate the NLC molecules and thus increase the refractive index when the initial $\hat{\mathbf{n}}$ is orthogonally aligned to the electric field [13]. Since large optical powers are never desirable as they could lead to heating, two main approaches can be adopted to overcome the optical Freédericksz threshold and adjust (maximize) the nonlinear reorientation. One is to pre-tilt the NLC molecules in the (Y, Z) plane at an angle θ_0 with respect to the Z direction by the application of an external low-frequency electric field E_{LF}, so that milliwatt power beams can rotate the molecular director $\hat{\mathbf{n}}$ and induce self-focusing [14]. A typical planar glass cell for the study of NLC solitary waves in the presence of an external voltage bias is sketched in Fig. 1(a); in this case a small pre-orientation $\delta\theta_0$ of the order of $1°$–$2°$ is ensured when the planar surfaces are treated for molecular anchoring in order to overcome the electric Freédericksz transition. The alternative method is to chemically treat or mechanically rub the planar walls of the cell (parallel to the (Y, Z) plane in Fig. 1) so that the NLC molecules are anchored at a given orientation θ_0 with respect to Z. Elastic forces then transfer the rotation into the bulk of the fluid dielectric, providing the homogeneous orientation of the sample. A beam propagating through the NLC and polarized with electric field in the principal (Y, Z) plane can then reorient the molecules by an additional angle ϕ from the pre-tilt, so that the total orientation of the molecular director to Z becomes $\theta = \theta_0 + \phi$. With

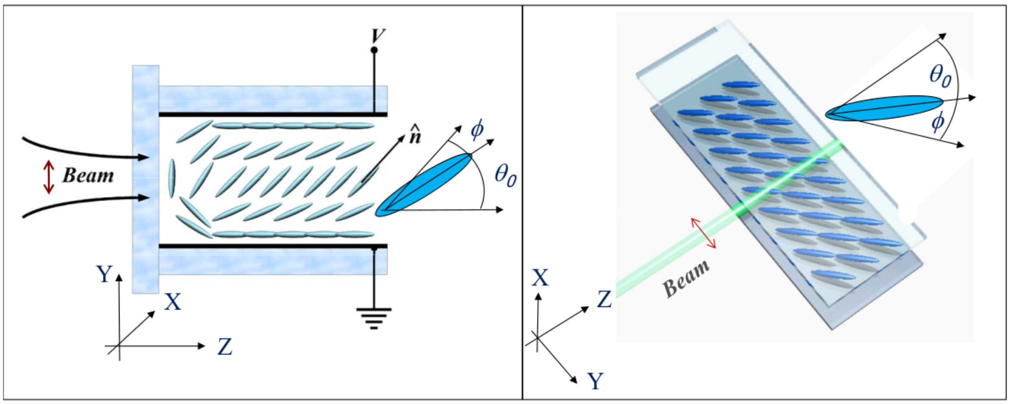

(a) (b)

Figure 1. Sketch of planar NLC glass cells in the two main configurations. (a) Biased cell: The orientation angle θ_0 is the pre-tilt induced by the external voltage V across the cell thickness and ϕ is the all-optical rotation of the induced dipoles (ellipses) in the plane of propagation (Y, Z). $\hat{\mathbf{n}}$ is the molecular director (optic axis) parallel to the long axis of the elongated NLC molecules. (b) Bias-free cell: the background orientation θ_0 is obtained by anchoring the molecular director at the planar boundaries parallel to (Y, Z). In both arrangements (a) and (b) the input light beam undergoing nonlinear reorientation is an extraordinary-wave launched from the left with electric field (double red arrow) polarized in the principal plane (Y, Z).

these assumptions and in the paraxial, slowly varying envelope approximation, the dimensional equations governing the propagation of an extraordinarily polarized light beam (electric field in the (Y, Z) plane) in a biased NLC sample (Fig. 1(a)) can be cast as [7,8,33]

$$2ik_0 n_e \frac{\partial E}{\partial Z} + 2ik_0 n_e \Delta \frac{\partial E}{\partial Y} + \nabla^2 E$$
$$+ k_0^2 \left[n_\perp^2 \cos^2\theta + n_\parallel^2 \sin^2\theta - n_\perp^2 \cos^2\theta_0 - n_\parallel^2 \sin^2\theta_0 \right] E = 0, \tag{1}$$

for the electric field of the beam and

$$K\nabla^2\phi + \left[\frac{1}{4}\epsilon_0 \Delta\epsilon |E|^2 + \frac{1}{2}\Delta\epsilon_{LF} E_{LF}^2 \right] \sin 2(\theta_0 + \phi) = 0, \tag{2}$$

for the reorientational nonlinearity [7,8,16,33]. Here, the θ-dependent extraordinary refractive index of the NLC is

$$n_e = \left[\frac{n_\perp^2 n_\parallel^2}{n_\parallel^2 \cos^2\theta + n_\perp^2 \sin^2\theta} \right]^{1/2}. \tag{3}$$

An extraordinary wave undergoes walkoff of the Poynting vector, so that the energy flux propagates in the (Y, Z) plane at an angle $\delta = \tan^{-1}\Delta$ to the wavevector (i. e., the Z direction in Fig. 1), where Δ is given by

$$\Delta = \frac{\Delta\epsilon \sin 2\theta}{\Delta\epsilon + 2n_\perp^2 + \Delta\epsilon \cos 2\theta}. \tag{4}$$

In the above equations, $\Delta\epsilon = n_\parallel^2 - n_\perp^2$ is the optical anisotropy, $\Delta\epsilon_{LF}$ is the low-frequency dielectric anisotropy and ϵ_0 is the electrical permittivity of free space. In addition, K is the elastic (Frank) constant in the scalar approximation for which the strengths of bend, twist and splay deformations are taken equal [7,13]. Finally, the Laplacians $\nabla^2 E$ and $\nabla^2\phi$ are in the transverse coordinates (X, Y).

The NLC equations (1) and (2) are highly nonlinear and so difficult to analyse. However, for continuous-wave milliwatt power beams the light-induced response ϕ is small, $|\phi| \ll |\theta_0|$, so that the model can be expanded in Taylor series around θ_0. In addition, these equations can be recast in a dimensionless form to reduce the number of parameters involved by using typical length scales L_Z and W down and across the cell, respectively, as well as an amplitude scale A_b for the electric field of the beam. Then

$$Z = L_Z z, \quad X = Wx, \quad Y = Wy, \quad E = A_b u. \tag{5}$$

Here, (x, y, z) is the non-dimensional coordinate system and u is the non-dimensional electric field of the beam. Suitable scales are [8,34]

$$L_Z = \frac{4n_e}{k_0 \Delta\epsilon \sin 2\theta_0}, \quad W = \frac{2}{k_0\sqrt{\Delta\epsilon \sin 2\theta_0}}, \quad A_b^2 = \frac{2P_b}{\pi\Gamma W_b^2}, \quad \Gamma = \frac{1}{2}\epsilon_0 c n_e \tag{6}$$

based on a Gaussian input wavepacket of power P_b, amplitude A_b and width W_b. The simplified non-dimensional equations governing beam propagation and the NLC response become

$$i\frac{\partial u}{\partial z} + i\gamma\Delta(\theta_0 + \phi)\frac{\partial u}{\partial y} + \frac{1}{2}\nabla^2 u + 2\phi u = 0, \tag{7}$$

$$\nu\nabla^2\phi - 2q\phi = -2|u|^2. \tag{8}$$

Here, the dimensionless elasticity ν and pre-tilt parameter q (when present) are given by

$$\nu = \frac{8K}{\epsilon_0 \Delta\epsilon A_b^2 W^2 \sin 2\theta_0} = \frac{\pi k_0^2 K \Gamma W_b^2}{\epsilon_0 P_b}, \quad q = \frac{4\Delta\epsilon_{LF} E_{LF}^2 \cos 2\theta_0}{\epsilon_0 \Delta\epsilon A_b^2 \sin 2\theta_0}. \tag{9}$$

Finally, the non-dimensional walkoff factor γ is

$$\gamma = \frac{2n_e}{\sqrt{\Delta\epsilon \sin 2\theta_0}}. \tag{10}$$

Note that the bias-free case (Fig. 1(b)) corresponds to $q = 0$. The model (7) and (8) is a focusing nonlocal, nonlinear Schrödinger (NLS) equation-type system with a refractive index increasing with the intensity $|u|^2$. Typical (reference) experimental values are a beam with power $P_b = 2mW$, half-width $W_b = 1.5\mu m$ and wavelength $\lambda_0 = 1.064\mu m$ in the near infrared for which Rayleigh scattering (intrinsic to NLC, [13]) is lower [7,8]. For the standard NLC mixture E7, the elastic constant is $K = 1.2 \times 10^{-11}N$. These parameters give an elasticity $\nu = O(100)$, as in previous studies [8,35,36]. The high value of ν indicates that the medium is operating in the highly nonlocal regime, in that the elastic response of the NLC to light extends far beyond the beam waist [7,16,33]. Noteworthy, beams governed in $(2+1)$ dimensions by local NLS models are unstable and undergo catastrophic collapse above a critical power [6]. However, a nonlocal response with a large ν can stabilize $(2+1)$-dimensional light beams [7,8,16,33] because the NLC equation (2) is elliptic and so its solution depends on u in the entire domain. This mathematical argument pairs with the physical concept of nonlocality due to the elastic response of soft matter.

It is of interest to note that equations of the same form as (7) and (8) arise in other areas in nonlinear optics and physics. Beam propagation in thermo-optic media is governed by the nematic system with $q = 0$ [37], e.g., in self-focusing lead glass [38,39] and colloidal suspensions with nano-particles to enhance light absorption [40]. Finally, systems of equations resembling the NLC model (7) and (8) apply to astrophysics. Such systems include the Schrödinger-Newton equations, which are a simple model of quantum gravitation [41,42]. Solitary wave solutions of the Schrödinger-Poisson system, i. e., the NLC model with $q = 0$ in the director equation (8), have been used to describe dark matter [43–45], the interaction between ordinary and dark galactic matter [46,47], N body systems of identical bosons with nonlocal interactions and dilute cold atom Bose-Einstein condensates, plasmas, electrons in semiconductors or metallic structures and water wave theory [43,48–50]. It should be noted that the NLC model (7) and (8) with $q \neq 0$ applies when the effect of boundary conditions in a finite thermo-optic cell is accounted for through the incorporation of a screened potential [43]. The Schrödinger-Newton equations also play a role in quantum hydrodynamics [43].

3. Interacting Beams

A simple manner in which to control a nematicon and its trajectory is to use a second one as a control beam, the interaction between the two being mediated by the nonlinear NLC response. Owing to the high nonlocality characterizing the medium, in fact, the wavepackets can "sense" one another without an apparent collision [51,52]. Let us first consider the interaction of two incoherent nematicons, with two non-interfering beams of electric fields u and v in relative proximity; neglecting walkoff, the NLC equations (7) and (8) can be extended to [53]

$$i\frac{\partial u}{\partial z} + \frac{1}{2}D_u\nabla^2 u + 2A_u\phi u = 0, \tag{11}$$

$$i\frac{\partial v}{\partial z} + \frac{1}{2}D_v\nabla^2 v + 2A_v\phi v = 0, \tag{12}$$

$$\nu\nabla^2\phi - 2q\phi = -2A_u|u|^2 - 2A_v|v|^2. \tag{13}$$

If the two beams share the same wavelength, then the diffraction coefficients can be scaled to $D_u = D_v = 1$, as can the coupling coefficients $A_u = A_v = 1$ [51,53].

The simplest collisional case is in-plane interactions [51,52,54–60], with solitary waves attracting and periodically interleaving as they propagate in the principal plane. While stable, steady multipole vector solitary waves can exist if the nonlocality ν is large enough [55,56], in most other cases the long range attraction mediated by the medium results in the beams oscillating about each other in the plane, irrespective of their relative phase, at variance with NLS solitary waves [52,54,61]. In the local limit $\nu \to 0$, the coupled NLC equations (11)–(13) reduce to coupled NLS equations. In-phase NLS solitary waves attract and out-of-phase NLS solitary waves repel [6], so the high nonlocality of NLC results in a significantly modified behaviour.

The in-plane interaction of nematicons can be modelled using modulation theory, with good agreement with full numerical solutions of the coupled nematic equations (11)–(13), a notable exception being the period of oscillation of the beams about each other [51,57]. This period difference greatly affects the beam phase for increasing z. A major result of this modelling is that nematicon trajectories are essentially determined by momentum conservation. Moreover, in the highly nonlocal limit, nematicons shed minimal radiation as they evolve [62], contributing minimal momentum to diffractive radiation. Although standard MT approximates solitary waves as point particles interacting under a potential [12], this was also extended to account for the non-point form of solitary waves [63], resulting in improved agreement with numerical solutions, albeit at the cost of increased complexity in the derivation of the MT equations and the equations themselves.

As nematicons propagate in the bulk of a thick planar cell, typically with $100\mu m$ between parallel glass plates, two interacting nematicons of equal power and size can spiral about each other and form a rotating cluster in three dimensions, exhibiting angular momentum as a whole due to their nonlocal interaction via the NLC [54,64–66]. Spiralling nematicons can be generated by the initial conditions

$$u = a_u f(\rho_u)\, e^{i\psi_u}, \quad v = a_v f(\rho_v)\, e^{i\psi_v}, \tag{14}$$

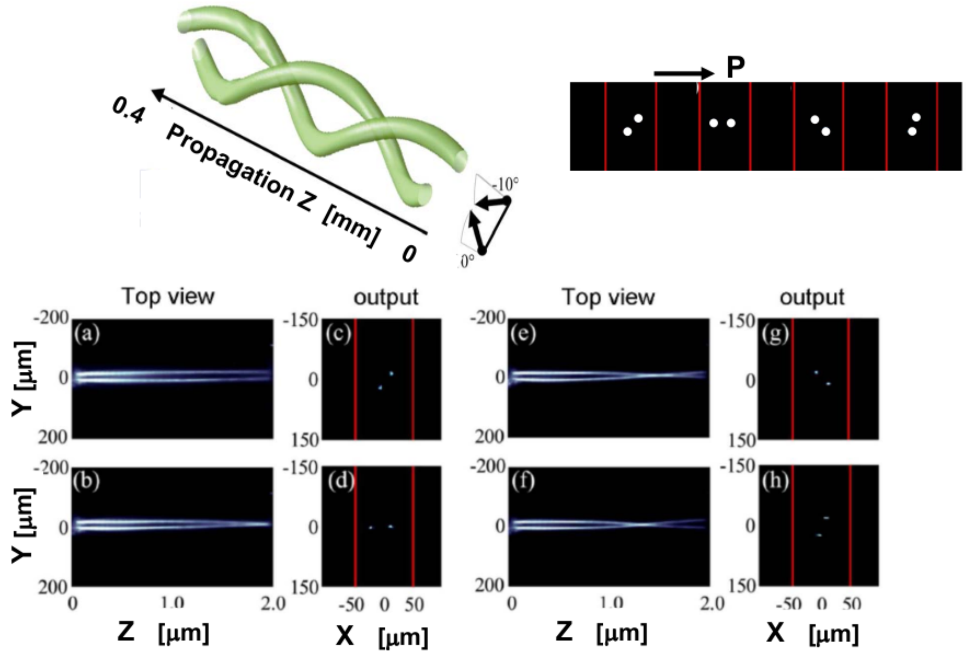

Figure 2. Spiralling nematicons. The NLC planar cell is realized as in Fig. 1(b). Top left: Numerical solution of nematic model (11)–(13) illustrating the mutual spiralling of two identical skew nematicons launched out-of-plane (Y, Z). Top right: Artist's rendering of the beam spots rotating about one another at the end of the sample for increasing excitation. (a)–(h): Experimental results; (a)–(b)–(e)–(f) Acquired images of beam evolution in (Y, Z) and (c)–(d)–(g)–(h) of the solitary wave cluster in the transverse plane (X, Y) at the sample output, for input powers 2.1, 2.7, 3.3 and 3.9 mW, respectively.

where

$$\rho_u = \frac{\sqrt{(x-\xi_u)^2 + (y-\eta_u)^2}}{w_u}, \qquad \rho_v = \frac{\sqrt{(x-\xi_v)^2 + (y-\eta_v)^2}}{w_v},$$
$$\psi_u = \sigma_u + U_u(x-\xi_u) + V_u(y-\eta_u), \qquad \psi_v = \sigma_v + U_v(x-\xi_v) + V_v(x-\eta_v) \quad (15)$$

at $z = 0$ in the two colour NLC equations (11)–(13), where f is the electric field profile of the beams, noting that the input wavepackets are usually Gaussian. The variables (U_u, V_u) and (U_v, V_v) are related to the angles at which the beams are inputted into the nematic cell and can be considered the input (x, y) "velocities" of the beams, with (ξ_u, η_u) and (ξ_v, η_v) the input positions of the beams. The spiralling of two skew nematicons about each other due to nonlocal, nonlinear attraction is illustrated in Fig. 2. This figure shows experimental results for two identical solitary waves launched and evolving out-of-plane and spiralling about one another for various input powers. The interacting beams are imaged in the observation plane (Y, Z), their output spots in the (X, Y) plane (Figs. 2(c), (d), (g) and (h)) at the end of the sample after they evolved in the down cell Z direction. The output spots appear to rotate as the beam power goes up and the effective angular momentum of the "two nematicon molecule" cluster increases, with an augmented angular velocity [64].

Nematicon spiralling was theoretically investigated using MT based on the input beams (14) [66]. Both beam profiles were either Gaussian, $f(\rho) = \exp(-\rho^2)$, or sech, $f(\rho) = \operatorname{sech}\rho$. Good to excellent agreement was obtained between full numerical solutions of the NLC equations (11)–(13) and MT for the trajectories, with the Gaussian and sech profiles providing comparable results in the highly nonlocal limit, the agreement improving for increasing angular momentum of the input cluster [66].

These findings confirmed that, in the highly nonlocal limit, nematicon trajectories are weakly dependent on the initial wavepacket profile [51,67]. It is important to underline that besides those based on the full nonlocal response of NLC, some studies rely on simplified models as the NLC equation (13) can be solved in terms of a Green's function G as

$$\phi = -2\int\int_{\text{cell}} G(x-x',y-y')\left[A_u|u(x',y',z)|^2 + A_v|v(x',y',z)|^2\right]dx'dy'. \tag{16}$$

Since in $(2+1)$ dimensions the Green's function G is the modified Bessel function of order 0, K_0, in general the solution (16) is not useful for analytical studies. For this reason, much work on light beam propagation in nonlocal, nonlinear media has adopted simplified responses for G, the most common being Gaussian and exponential. Of particular relevance to the present review, the in-plane interaction of two solitary waves was investigated by means of a Gaussian [68,69] and an exponential response [70], and their spiralling with a Gaussian [71]; such studies were in qualitative agreement with those based on the actual NLC response.

At the end of this section, we deem appropriate to mention that a range of experimental and numerical studies were undertaken of self-guided beams interacting in other nonlocal media [72], particularly those with a self-focusing thermo-optic response [39,73]. The understanding and intuitive perception of nonlinear phenomena in reorientational soft matter, in fact, may benefit from the insight afforded by solitary waves in thermal media. For the latter scenario the governing equations are the Schrödinger-Poisson model (7) and (8), where ϕ denotes the temperature, with the walk-off factor and the pre-tilt set to zero, $\gamma = 0$ and $q = 0$. Employing lead-glass, it was reported in [39] that in $(1+1)$D two propagating solitary waves attract each other; in $(2+1)$D spiralling can occur, with orbits dependent on the nonlocality. In local media the orbits of two interacting beams are elliptical, whereas in nonlocal media circular orbits, with tangential velocity independent of separation, are possible. The final comment is that the trajectories of the interacting nematicons can be controlled and varied by adjusting the separation and power of the beams.

4. Refraction and Reflection of Self-Guided Beams at Interfaces

A basic topic in optics is the refraction of plane waves of light at the interface between two dielectrics of different refractive indices, governed by Snell's Law in the linear regime. Nematicons can be similarly refracted at interfaces which delineate NLC regions with different background orientations of the optic axis, resulting in unequal refractive indices. However, in spite of their particle-like behaviour resembling plane waves with a principal wavevector, since nematicons are extended nonlinear wavepackets in a nonlinear medium, their refraction and reflection can depart from those of linear light beams [74].

Let us assume that two external low frequency electric fields (voltages) are applied across two regions of a planar NLC cell, as in the experiments of [28], and as sketched in the top panel of Figure 3. Two sets of electrodes apply the two bias voltages and are separated along the line $y = \mu_1 z + \mu_2$, so that the beams refract in the (y, z) plane. The two biases generate a background director orientation ϕ_b which consists of the angle ϕ_{bl} to the left and ϕ_{br} to the right of the interface, respectively. The non-dimensional NLC equations (7) and (8) are then modified to [28,75]

$$\begin{aligned} i\frac{\partial u}{\partial z} + i\gamma\Delta(\phi_b)\frac{\partial u}{\partial y} + \frac{1}{2}\nabla^2 u + \sin(2\phi_b)\phi u &= 0 && (17)\\ \nu\nabla^2\phi - 2q\phi &= -\sin(2\phi_b)|u|^2. && (18)\end{aligned}$$

Here,

$$\phi_b = \begin{cases} \phi_{bl}, & \mu_1 z + \mu_2 < y, \\ \phi_{br}, & y < \mu_1 z + \mu_2 \end{cases} \tag{19}$$

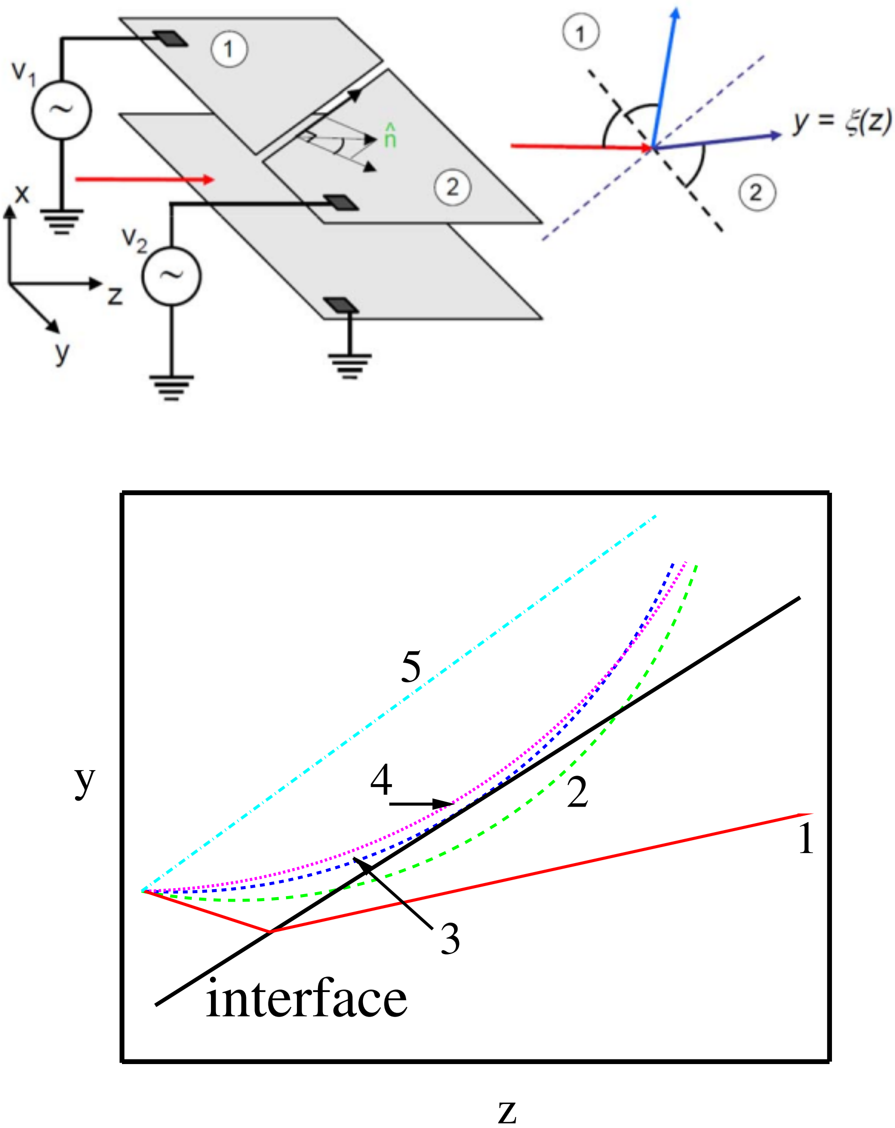

Figure 3. Top: Sketch of nematic cell with dielectric interface. The two regions of different refractive indices are generated by two external voltages V_1 and V_2 applied across isolated sections of the cell. The right sketch shows the incident (red), refracted (purple) and reflected (light blue) nematicons at the interface. The beam path in the (y,z) plane is $y = \xi(z)$. Bottom: Refraction/reflection of a nematicon at a dielectric interface in NLC. The beam propagates from a more to a less optically dense NLC region. 1. refraction: solid red line, 2. Goos-Hänchen type reflection: long-dash green line, 3. total internal reflection with beam axis tangential at the interface: short-dash dark-blue line, 4. total internal reflection with beam axis in the denser medium: dotted pink line, 5. straight beam path: dash-dot light-blue line. The interface is indicated by the thick straight solid line in black.

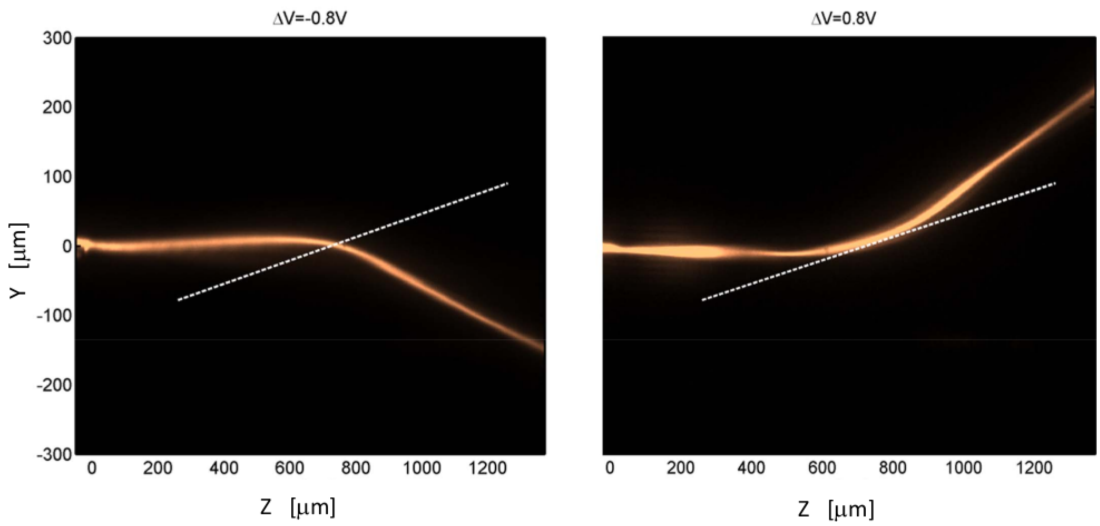

Figure 4. Observation of a near-infrared 4.5 mW nematicon interacting with a voltage controlled dielectric interface in NLC as it travels from the left to the right. Left: Refraction of the nematicon going towards a denser region; Right: total internal reflection of the nematicon propagating towards a less dense region at an incidence angle exceeding the critical value. The opposite values of the applied voltage difference ΔV marked above the panels are consistent with the opposite refractive index contrast imposed between the two dielectric regions in the two cases. Reproduced with permission from Springer Nature. All rights reserved. [28], doi: https://doi.org/10.1038/nphys427

and the non-dimensional bias q is

$$q = \begin{cases} q_l, & \mu_1 z + \mu_2 < y, \\ q_r, & y < \mu_1 z + \mu_2, \end{cases} \tag{20}$$

see (9) and the top panel of Figure 3. Note that the basic nematic equations (7) and (8) were modified as the background director orientation in the absence of the optical beam is now non-uniform, resulting in the $\sin 2\phi_b$ coefficients which cannot be scaled out.

For linear propagation from a more to a less optically dense medium, a light beam either refracts or undergoes total internal reflection (TIR). The refraction of a nematicon travelling from higher to lower refractive index regions shows a similar behaviour, but has to account for the nonlinear, extended profile of a self-guided solitary wave. Various cases of nematicons at the interface are illustrated in the bottom panel of Fig. 3 with the lines plotting the center-of-mass of the propagating wavepacket (see [75]). The usual Snell's Law refraction is type 1. For angles of incidence larger than a critical value the nematicon undergoes TIR, types 2, 3 and 4. Type 3 is equivalent to linear TIR, with the beam reflected with its centre tangential at the interface. However, since the nematicon transverse profile can exist on both sides of the interface, the beam can penetrate the less optically dense region, turn around and re-enter the denser NLC: this is denoted as Goos-Hänchen TIR [76] in Fig. 3. Reflection type 4 illustrates TIR for which the nematicon bends towards the incidence region without its centre 'touching' the interface, whilst its tail enters the less dense region. Figure 4 shows experimental results for the refraction from a less to a more optically dense medium and total internal reflection from a less to a more optically dense medium of a nematicon at an interface to illustrate these refraction and reflection regimes. The refraction of a nematicon going from a less to a more optically dense NLC region resembles that of linear waves [28,75].

Modulation theory was developed to model nematicon refraction at interfaces, as governed by the NLC equations (17) and (18) [75,77]. This model essentially treats the nematicon as an equivalent particle in a varying medium (mechanical potential) [12,78], the essential concept behind the term "soliton." This work [75,77] found excellent agreement between these MT solutions and full numerical solutions of (17) and (18), including the incidence angles separating the various refraction and reflection types illustrated in Fig. 3. The pertinent initial conditions for this MT model are

$$u = a \operatorname{sech} \frac{\sqrt{x^2 + (y-\xi)^2}}{w} e^{i\sigma + iU(y-\xi)}, \quad \phi = \alpha \operatorname{sech}^2 \frac{\sqrt{x^2 + (y-\xi)^2}}{\beta}. \tag{21}$$

As for the initial condition (14) for spiralling nematicons, U is related to the input angle of the beam in the (y, z) plane and can be considered the input y "velocity" of the beam which is inputted at $x = 0$ and $y = \xi$ at $z = 0$.

The analysis of NLC self-confined beams refracting at an interface was further extended to optical vortex beams (i.e., propagating vortices rather than those discussed in [79]) based on the input wavepacket [80]

$$u = are^{-r/w} e^{i\sigma + iU(y-\xi) + i\varphi}, \tag{22}$$

which is a vortex of (topological) charge one [6], with (r, φ) being plane polar coordinates and U and ξ having the same meaning as for the nematicon initial condition (21). In local media optical vortices are unstable to a mode 2 azimuthal instability, but they stabilize in sufficiently nonlocal media, such as nematic liquid crystals [81–83] and thermo-optic media [73], including dye-doped NLC [84]. Optical vortices share similar refraction/reflection at a NLC dielectric interface as nematicons, including Snell's Law type and TIR. The major difference is that a vortex is less stable than a nematicon; hence, its deformation upon refraction can destabilise it, so that it easily breaks up into stable nematicons [80], as illustrated in Figure 5. This figure shows snapshot cross-sections in the (x, y) plane of the evolving vortex at various downcell distances z as it crosses the refractive index interface given by (19) and (20). The deformation of a vortex hitting the interface is clearly visible in Fig. 5(b), and increases as more of the vortex interacts with it, as in Fig. 5(c). This ultimately results in the destruction of the vortex, Figs. 5(d)–(f), and its break up into solitary waves. In later work it was found that the stability of an optical vortex propagating through a dielectric interface can be enhanced by a co-propagating coaxial nematicon as the latter acts as a waveguide and helps to keep the vortex together by confining a large amount of its high amplitude field distribution [85].

As we did earlier, we note that self-focusing thermal media have also been exploited for analytical, numerical and experimental studies of solitary wave-vortex interactions. In [86–88] the authors used orthogonally polarized beams in a cylindrical medium, illustrating the propagation of a coupled bell-shape beam with a higher-order ring or doughnut-like vortex. At a critical power ratio stationary vector solitary waves can be excited, as confirmed by experiments in lead glass [86–88].

5. Interaction of Localised Beams with Dielectric Perturbations

The trajectories of optical solitary waves in NLC can also be manipulated by localised perturbations— defects— of the refractive index, acting in a manner similar to a lens [7,89,90]. There are a number of techniques to generate refractive defects as the orientation of NLC molecules, and so the refractive index, can be controlled via numerous mechanisms, including applied electric fields [21,25,28,30,91–93], dye-doping [26,94–97], polymer dispersion/doping [98,99], external magnetic fields [100–102], disinclinations and topological structures [103,104] and other (incoherent) light beams [22,24,26,89,105]. However, since a nematicon is a wavepacket with an extended profile, it can interact with the localised defect/lens even if its peak is somewhat distant from it, similar to the case of total internal reflection discussed in Section 4. As remarked before, NLC are a nonlocal, nonlinear medium for which the reorientation extends well beyond the beam waist forcing it. Let us consider a refractive perturbation of background director orientation $\phi_b(x, y, z)$ about the uniform pre-tilt θ_0 in a region denoted by Ω. As the director orientation is linked to the extraordinary refractive index n_e, see (3), a light beam

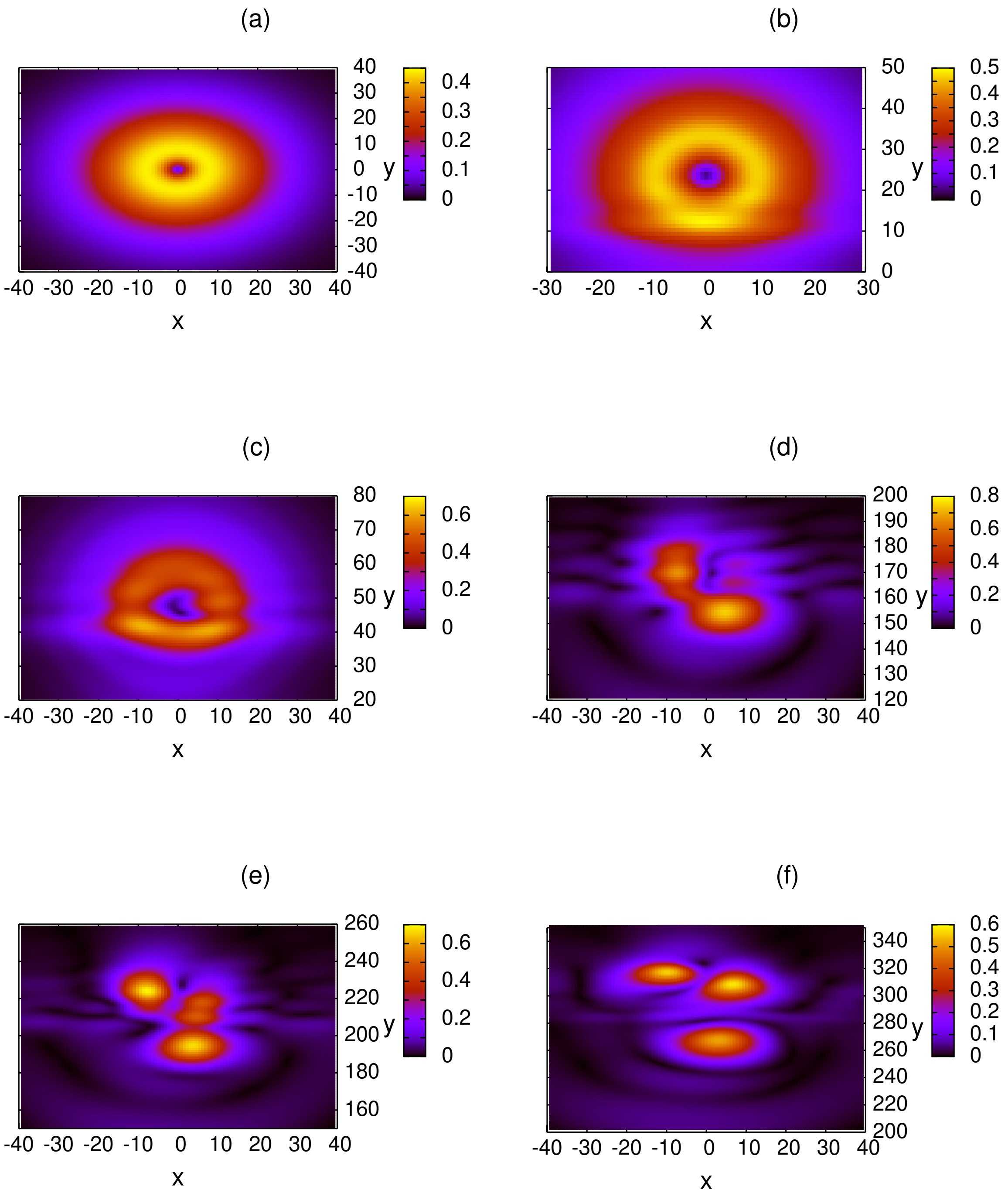

Figure 5. Transverse profiles of $|u|$ from the numerical solution of model (17) and (18) and the initial conditions (22) with $a = 0.15$, $w = 8.0$ and $V = 1.3$ at $z = 0$, with $\nu = 200$, $\psi_{bl} = 0.8$, $\psi_{br} = 0.4$, $q_l = 1.3$, $q_r = 1.0$, $\mu_1 = 1.5$ and $\mu_2 = -20$. (a) $z = 0$, (b) $z = 20$, (c) $z = 40$, (d) $z = 120$, (e) $z = 150$, (f) $z = 200$. The NLC cell is biased as in Fig. 1(a). [80], doi: http://dx.doi.org/10.1088/0953-4075/45/16/165403

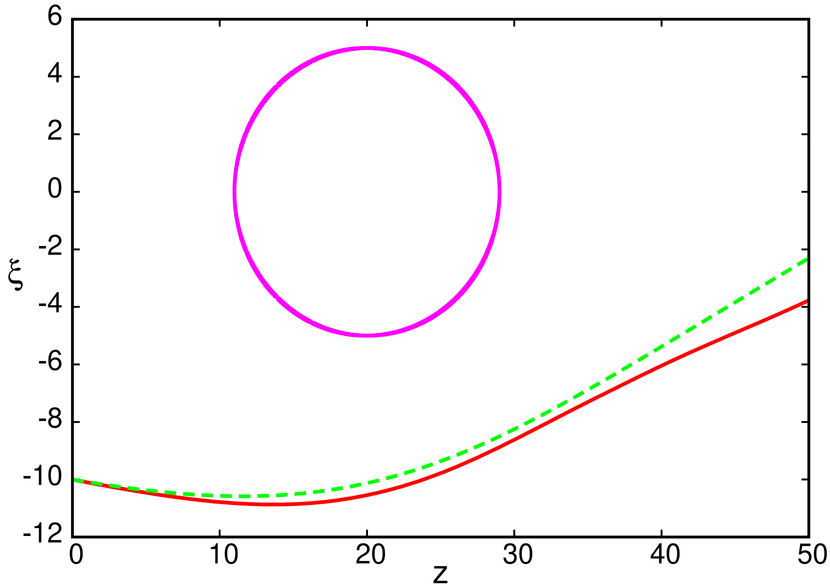

Figure 6. Comparison of nematicon trajectories $y = \xi(z)$ nearing an elliptical region Ω of differing refractive index in an NLC cell prepared as in Fig. 1(b). The initial condition is (25). Numerical solution of (23) and (24): red line; solution of MT equations [27]: dashed green line. The initial condition is $f(\rho) = \operatorname{sech}\rho$, $a = 2.5$, $w = 2.0$, $U = -0.1$, $\xi = -10.0$ with $\nu = 200$ and $q = 2$. The defect parameters are $u_0 = 1$, $Y_\Omega = 0$, $Z_\Omega = 20$ and $R_y = 5$, $R_z = 9$. The boundary of Ω is given by the pink line. Reproduced with permission from the American Physical Society. All rights reserved. [27], doi: http://dx.doi.org/10.1103/PhysRevA.82.053843

can be refracted when passing through, or near, such a localised defect in n_e and modify its trajectory. On adding this index perturbation, the NLC model (7) and (8) becomes

$$i\frac{\partial u}{\partial z} + i\gamma\Delta(\theta_0 + \phi_b)\frac{\partial u}{\partial y} + \frac{1}{2}\nabla^2 u + 2\phi_b u + 2\phi u = 0, \tag{23}$$

$$\nu\nabla^2\phi - 2q\phi = -2|u|^2. \tag{24}$$

Note that the nonlinear term in the electric field equation is of the form $\Delta n u$, where Δn is the light-induced change in refractive index from its pre-tilt value.

As stated above, the dielectric defect acts as a lens to modify the beam trajectory. Nematicon refraction by localised index perturbations induced by an external electric field (of constant value u_0 inside the region Ω and 0 otherwise) was studied by full numerical solutions of (23) and (24) and MT [27] using circular, elliptical and rectangular domains Ω. The input beam was taken as

$$u = af(\rho)e^{i\sigma + iU(y-\xi)}, \quad \rho = \frac{\sqrt{x^2 + (y-\xi)^2}}{w} \tag{25}$$

with profile $f(\rho)$ either Gaussian or sech, obtaining comparable results, as expected from previous studies on the role of the beam profile on nematicon propagation [67].

The example of an elliptical refractive index change can illustrate the findings in [27]. The defect can be generated by an applied low frequency electric field of the form

$$u_b = \begin{cases} u_0, & \Gamma = \frac{(y-Y_\Omega)^2}{R_y^2} + \frac{(z-Z_\Omega)^2}{R_z^2} \le 1, \\ 0, & \Gamma > 1, \end{cases} \tag{26}$$

providing the desired background orientation of the optic axis $\hat{\mathbf{n}}$. Figure 6 compares the nematicon trajectory $y = \xi(z)$ as given by full numerical solutions of the NLC model (23) and (24) with the initial condition (25) and by modulation theory. It can be seen that MT

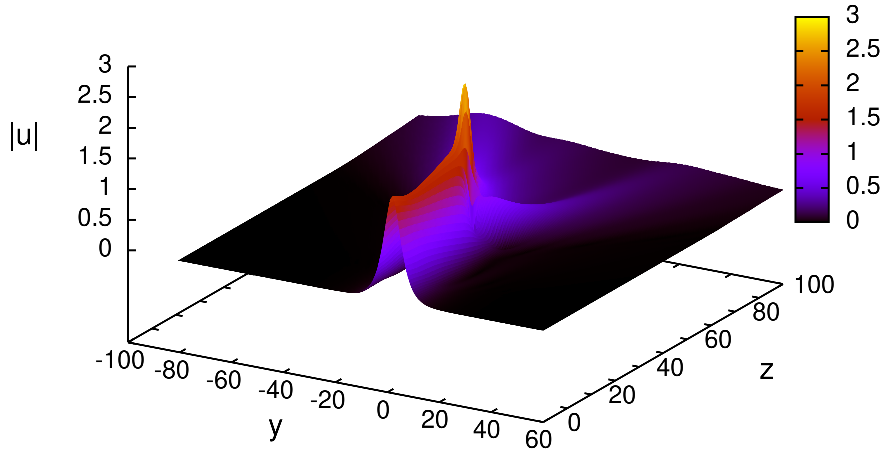

Figure 7. Evolution of $|u|$ in the plane $x = 0$ as given by numerical solution of equations (23) and (24) in a sample as in Fig. 1(b). The initial condition is (25) with $f(\rho) = \mathrm{sech}\,\rho$, $w = 3.0$, $U = -0.05$, $\xi = 2.0$ with $\nu = 400$ and $q = 2$. The defect parameters are $a_b = 0.5$, $w_b = 3.0$, $Y_b = 0$ and $Z_b = 30$. Reproduced with permission from the American Physical Society. All rights reserved. [106], doi: http://dx.doi.org/10.1103/PhysRevA.85.013804

gives a good prediction of the nematicon trajectory as it is refracted by the index change. These results show that the trajectory of a nematicon can be controlled by adjusting the strength of the dielectric defect, much as adjusting a lens controls the path of light.

The study of nematicon refraction in proximity to dielectric defects was extended to nematicon paths interacting with the perturbation itself [106], based on the assumed additional orientation

$$\theta_b = a_b e^{-\left[(y-Y_b)^2+(z-Z_b)^2\right]/w_b^2} \tag{27}$$

and the input wavepacket (25). If the beam waist is small compared with the defect width, then self-localisation is preserved and the solitary wave refracts much as for the case of propagation around the defect [27]. However, if the beam and defect have comparable sizes, then a large enough refractive index contrast can pull apart the nematicon, as apparent in Fig. 7, where the latter breaks up into two beams. These two beams are the counterparts of the caustics forming in the linear regime [106].

The work summarized above was extended to experimental and theoretical studies in unbiased planar samples with a background director orientation θ_0 varying across the transverse Y direction, but uniform in the down cell Z direction [107,108]. The NLC equations (23) and (24) govern such propagation with $q = 0$, since in the experiments [107] the NLC molecules were pre-tilted by the physical treatment of the glass plates (Fig. 1(b)). The modulation theory used to model the experiments was based on the beam and director distributions

$$\begin{aligned} u &= af(\rho)e^{i\sigma+iU(z)(y-\xi(z))}, \quad \rho = \frac{\sqrt{x^2+(y-\xi(z))^2}}{w} \\ \theta &= \alpha f^2(\mu), \quad \mu = \frac{\sqrt{x^2+(y-\xi(z))^2}}{\beta}. \end{aligned} \tag{28}$$

Here, a and w are the amplitude and width of the beam and α and β are the amplitude and width of the director response to the optical forcing. The variable $\xi(z)$ is the y position of the nematicon peak as it travels down the cell with z increasing, $y = \xi(z)$ as

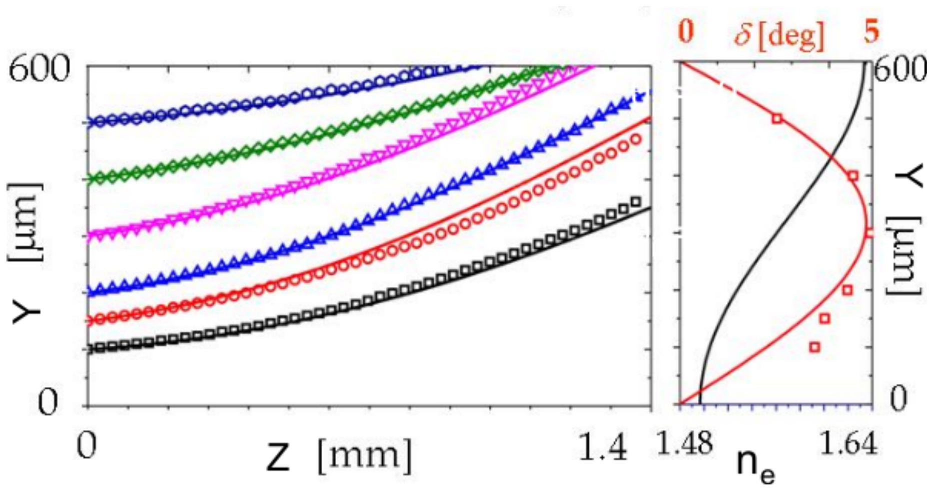

Figure 8. Left panel: Nematicon trajectories for an unbiased NLC sample (see Fig. 1(b)) with background angle θ_0 varying in Y from 0^o at $Y = 0\mu m$ to 90^o at $Y = 600\mu m$. Experimental data: symbols; MT results: solid lines. Right panel: Extraordinary refractive index n_e and walkoff angle $\delta = \tan^{-1}\Delta$ across nematic cell. The red squares are the experimentally measured walkoff. Reproduced with permission from Springer Nature. [107], doi: 10.1038/s41598-017-12242-5

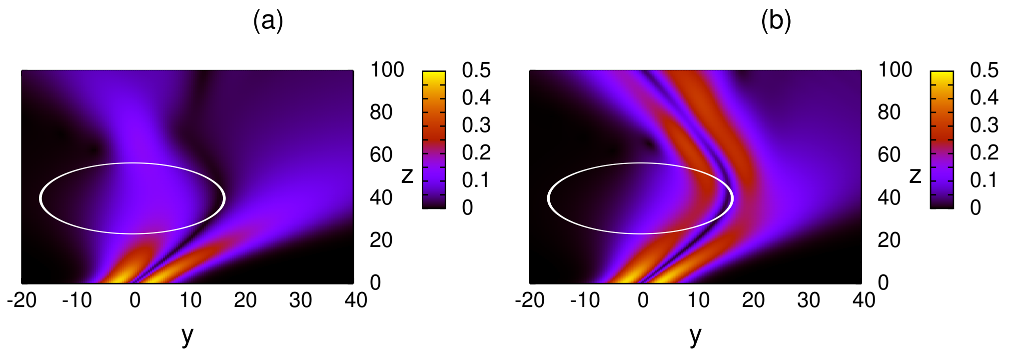

Figure 9. Evolution in $(x = 0, y, z)$ of coupled optical vortex and solitary wave near a Gaussian refractive defect (white ellipse) in an unbiased NLC sample. (a) Vortex beam alone and (b) vortex with co-propagating nematicon. Reprinted with permission from [113] ©The Optical Society.

it evolves in the (y, z) plane with fixed $x = 0$, and $U(z)$ is the nematicon y "velocity", physically the angle it makes with the z direction in the (y, z) plane. We underline that the beam profile is not specified above. It was found that if the length scale of the refractive index change is larger than the beam width, then the MT results are independent of the profile and the MT equations reduce to momentum conservation equations for the wavepacket trajectory $\xi(z)$, as for interacting nematicons [51]. This is important since, as stated in Section 4, there are no known exact nematicon solutions on which to base modulation theory. Fig. 8 compares experimental and MT results (momentum conservation) for the nematicon trajectory, with an excellent match. These investigations of nematicon refraction in a sample with a transverse varying background director orientation were also carried out in samples with background director distribution θ_0 varying longitudinally (in the down cell direction Z), with perfect agreement between measurements and MT results [109].

As discussed in Section 4, an optical vortex beam is a much less stable entity than a nematicon, so when it interacts with a dielectric defect it can be destabilised and break up into individual beams [80]. A co-propagating coaxial nematicon can stabilise an optical vortex in a uniform NLC sample, as demonstrated both experimentally [36] and theoretically [110,111], as was also found experimentally and theoretically for co-propagating solitary waves and optical vortices in thermal nonlinear optical media [86–88]. It was found that a refracting vortex can also be stabilised by a co-propagating co-polarized nematicon which acts as a graded-index waveguide and routes the vortex [112,113]. Fig. 9 illustrates the stabilising effect of such a coaxial nematicon on a vortex as the combined wavepackets propagate through an elliptically shaped dielectric defect of the form

$$\theta_b = a_b e^{-\left[(y-Y_b))^2+(z-Z_b)^2\right]/w_b^2}. \tag{29}$$

Figure 9(a) shows the evolution of a vortex beam (charge 1) alone: its destruction by way of the index defect can be clearly appreciated. Fig. 9(b) displays the evolution of the same vortex co-propagating with a co-polarized nematicon, resulting in vortex stabilisation despite its interaction with the defect.

6. Conclusions

In this review we have tried to present a descriptive synopsis of recent results on the study of interacting self-confined optical solitary waves in reorientational nematic liquid crystals, outlining the main analytical approaches based on modulation theory. Despite the non-exhaustive character of the review, it is apparent that nematicons and other solitary waves in this specific type of soft matter have triggered a conspicuous amount of research interest and scientific effort, stimulating the development of theoretical, numerical and experimental approaches motivated by the sensitivity of liquid crystals to quite diverse perturbations, from light to voltage, magnetic fields, temperature, doping, etc. Beyond the specific topics summarized hereby, additional and recent endeavours have been carried out at the frontiers of self-localized light in nematic liquid crystals, including, e. g., Pancharatnam-Berry geometric phase and spin-orbit (spin-optical) solitary waves [114–117], thermo-reorientational nonlinear competition and multi-hump supermode solitary waves [118–126], to cite a few. Such phenomena involve the interaction of optical solitary waves in NLC with polarization evolution and scattering, competing self-focusing and defocusing responses, etc. Given the resultant complexity, they seem to deserve their own dedicated review, which is underway.

Conflicts of Interest: The authors declare no conflict of interest.

References

1. J.S. Russell, "Report on waves," in: *14th Meeting of the British Association for the Advancement of Science*, John Murray, London, **1845**, 311–390.
2. G.B. Whitham, *Linear and Nonlinear Waves*, J. Wiley and Sons, New York, **1974**.
3. M.J. Ablowitz, *Nonlinear Dispersive Waves. Asymptotic Analysis and Solitons*, Cambridge University Press, Cambridge, **2011**.
4. G.P. Agrawal, *Nonlinear Fiber Optics*, Academic Press, San Diego, **1995**.
5. G.I. Stegeman, D.N. Christodoulides and M. Segev, "Optical spatial solitons: Historical perspectives," *IEEE J. Sel. Top. Quantum Electron.*, **2000**, *5*, 1419–1427.
6. Y.S. Kivshar and G.P. Agrawal, *Optical Solitons. From Fibers to Photonic Crystals*, Academic Press, San Diego, **2003**.
7. M. Peccianti and G. Assanto, "Nematicons," *Phys. Rep.*, **2012**, *516*, 147–208.
8. G. Assanto and N.F. Smyth, "Self-confined light waves in nematic liquid crystals," *Physica D*, **2020**, *402*, 132182.
9. A. Jeffrey, "Role of the Korteweg-de Vries equation in plasma physics," *Q. J. Roy. Astron. Soc.*, **1973**, *14*, 183–189.
10. A.S. Davydov, *Solitons in Molecular Systems*, 2nd ed. Kluwer Academic Publishers, Dordrecht, **1991**.
11. M. Tlidi, K. Staliunas, K. Panajotov, A.G. Vladimirov and M.G. Clerc, "Localized structures in dissipative media: from optics to plant ecology," *Phil. Trans. R. Soc. A*, **2014**, *372*, 20140101.
12. D.J. Kaup and A.C. Newell, "Solitons as particles, oscillators, and in slowly changing media: a singular perturbation theory," *Proc. Roy. Soc. Lond. A*, **1978**, *361*, 413–446.
13. I.C. Khoo, *Liquid Crystals*, Wiley, New York, **2022**.
14. M. Peccianti, G. Assanto, A. De Luca, C. Umeton and I.C. Khoo, "Electrically assisted self-confinement and waveguiding in planar nematic liquid crystal cells," *Appl. Phys. Lett.*, **2000**, *77*, 7–9.
15. G. Assanto and M. Karpierz, "Nematicons: self-localized beams in nematic liquid crystals," *Liq. Cryst.*, **2009**, *36*, 1161–1172.
16. G. Assanto, "Nematicons: reorientational solitons from optics to photonics," *Liq. Cryst. Rev.*, **2018**, *6*, 170–194.

17. G. Assanto and M. Peccianti, "Spatial solitons in nematic liquid crystals," *IEEE J. Quantum Electron.*, **2003**, *39*, 13–21.
18. G. Assanto, A.A. Minzoni and N.F. Smyth, "Light self-localization in nematic liquid crystals: modelling solitons in nonlocal reorientational media," *J. Nonl. Opt. Phys. Mat.*, **2009**, *18*, 657–691.
19. A. Alberucci, G. Assanto, J.M.L. MacNeil and N.F. Smyth, 2014, "Nematic liquid crystals: an excellent playground for nonlocal nonlinear light localization in soft matter," *J. Nonl. Opt. Phys. Mat.*, **2014**, *23*, 1450046.
20. M. Peccianti, C. Conti, G. Assanto, A. de Luca and C. Umeton, "All-optical switching and logic gating with spatial solitons in liquid crystals," *Appl. Phys. Lett.*, **2002**, *81*, 3335–3337.
21. M. Peccianti, C. Conti, G. Assanto, A. de Luca and C. Umeton, "Routing of anisotropic spatial solitons and modulational instability in liquid crystals," *Nature*, **2004**, *432*, 733–737.
22. S.V. Serak, N.V. Tabiryan, M. Peccianti and G. Assanto, "Spatial soliton all-optical logic gates" *IEEE Photon. Tech. Lett.*, **2006**, *18*, 1287–1289.
23. M. Peccianti, A. Dyadyusha, M. Kaczmarek and G. Assanto, "Escaping solitons from a trapping potential," *Phys. Rev. Lett.*, **2008**, *101*, 153902.
24. A. Piccardi, G. Assanto, L. Lucchetti and F. Simoni, "All-optical steering of soliton waveguides in dye-doped liquid crystals," *Appl. Phys. Lett.*, **2008**, *93*, 171104.
25. A. Alberucci, A. Piccardi, U. Bortolozzo, S. Residori and G. Assanto, "Nematicon all-optical control in liquid crystal light valves," *Opt. Lett.*, **2010**, *35*, 390–392.
26. A. Piccardi, A. Alberucci, U. Bortolozzo, S. Residori and G. Assanto, "Soliton gating and switching in liquid crystal light valve," *Appl. Phys. Lett.*, **2010**, *96*, 071104.
27. G. Assanto, A.A. Minzoni, N.F. Smyth and A.L. Worthy, "Refraction of nonlinear beams by localised refractive index changes in nematic liquid crystals," *Phys. Rev. A*, **2010**, *82*, 053843.
28. M. Peccianti, A. Dyadyusha, M. Kaczmarek and G. Assanto, "Tunable refraction and reflection of self-confined light beams," *Nature Phys.*, **2006**, *2*, 737–742.
29. A. Piccardi, A. Alberucci, N. Kravets, O. Buchnev and G. Assanto, "Power controlled transition from standard to negative refraction in reorientational soft matter," *Nat. Commun.*, **2014**, *5*, 5533–5541.
30. S. Perumbilavil, A. Piccardi, R. Barboza, O. Buchnev, G. Strangi, M. Kauranen and G. Assanto, "Beaming random lasers with soliton control," *Nat. Commun.*, **2018**, *9*, 3863, 1–7.
31. J.M.L. MacNeil, N.F. Smyth and G. Assanto, "Exact and approximate solutions for solitary waves in nematic liquid crystals," *Physica D*, **2014**, *284*, 1–15.
32. B. Malomed, "Variational methods in nonlinear fiber optics and related fields," *Prog. Opt.*, **2002**, *43*, 71–193.
33. C. Conti, M. Peccianti and G. Assanto, "Route to nonlocality and observation of accessible solitons," *Phys. Rev. Lett.*, **2003**, *91*, 073901.
34. C. García-Reimbert, A.A. Minzoni, N.F. Smyth and A.L. Worthy, "Large-amplitude nematicon propagation in a liquid crystal with local response," *J. Opt. Soc. Amer. B*, **2006**, *23*, 2551–2558.
35. G. Assanto, A. A. Minzoni, M. Peccianti and N. F. Smyth, "Optical solitary waves escaping a wide trapping potential in nematic liquid crystals: modulation theory," *Phys. Rev. A*, **2009**, *79*, 033837.
36. Y. Izdebskaya, W. Krolikowski, N.F. Smyth and G. Assanto, "Vortex stabilization by means of spatial solitons in nonlocal media," *J. Opt.*, **2016**, *18*, 054006.
37. E.A. Kuznetsov and A.M. Rubenchik, "Soliton stabilization in plasmas and hydrodynamics," *Phys. Rep.*, **142**, 103–165 (1986).
38. F.W. Dabby and J.R. Whinnery, "Thermal self-focusing of laser beams in lead glasses," *Appl. Phys. Lett.*, **13**, 284–286 (1968).
39. C. Rotschild, B. Alfassi, O. Cohen and M. Segev, " Long-range interactions between optical solitons," *Nat. Phys.*, **2006**, *2*, 769-774.
40. M.Y. Salazar-Romero, Y.A. Ayala, E. Brambila, L.A. Lopez-Peña, L. Sciberras, A.A. Minzoni, R.A. Terborg, J.P. Torres and K. Volke-Sepúlveda, "Steering and switching of soliton-like beams via interaction in a nanocolloid with positive polarizability," *Opt. Lett.*, **2017**, *42*, 2487–2490.
41. R. Penrose, "Quantum computation, entanglement and state reduction," *Phil. Trans. R. Soc. Lond. A*, **1998**, *356*, 1927–1939.
42. I.M. Moroz, R. Penrose and P. Tod, "Spherically-symmetric solutions of the Schrödinger-Newton equations," *Class. Quan. Gravity*, **1998**, *15*, 2733–2742.
43. A. Paredes, D.N. Olivieri, H. Michinel, "From optics to dark matter: A review on nonlinear Schrödinger–Poisson systems," *Physica D*, **2020**, *403*, 132301.
44. A.H. Guth, M.P. Hertzberg and C. Prescod-Weinstein, "Do dark matter axions form a condensate with long-range correlation?", *Phys. Rev. D*, **2015**, *92*, 103513.
45. L. Hui, J.P. Ostriker, S. Tremaine and E. Witten, "Ultralight scalars as cosmological dark matter," *Phys. Rev. D*, **2017**, *95(4)*, 043541.
46. A. Paredes and H. Michinel, "Interference of dark matter solitons and galactic offsets," *Phys. Dark Universe*, **2016**, *12*, 50–55.
47. A. Navarrete, A. Paredes, J.R. Salgueiro and H. Michinel, "Spatial solitons in thermo-optical media from the nonlinear Schrödinger-Poisson equation and dark-matter analogues," *Phys. Rev. A*, **2017**, *95*, 013844.
48. A. Davey and K. Stewartson, "On three-dimensional packets of surface waves," *Proc. R. Soc. Lond. Ser. A Math. Phys. Eng. Sci.*, **1974**, *338*, 101–110.
49. N. Freeman and A. Davey, "On the evolution of packets of long surface waves," *Proc. R. Soc. Lond. Ser. A Math. Phys. Eng. Sci.*, **1975**, *344*, 427–433.

50. I. Ioannou-Sougleridis, D.J. Frantzeskakis, T.P. Horikis, "A Davey-Stewartson description of two-dimensional solitons in nonlocal media," *Stud. Appl. Math.*, **2019**, *144*, 3–17.
51. B.D. Skuse and N.F. Smyth, "Interaction of two colour solitary waves in a liquid crystal in the nonlocal regime," *Phys. Rev. A*, **2009**, *79*, 063806.
52. M. Peccianti, K.A. Brzdiąkiewicz and G. Assanto, "Nonlocal spatial soliton interactions in nematic liquid crystals," *Opt. Lett.*, **2002**, *27*, 1460–1462.
53. A. Alberucci, M. Peccianti, G. Assanto, A. Dyadyusha and M. Kaczmarek, "Two-color vector solitons in nonlocal media," *Phys. Rev. Lett.*, **2006**, *97*, 153903.
54. A. Fratalocchi, M. Peccianti, C. Conti and G. Assanto, "Spiralling and cyclic dynamics of nematicons," *Mol. Cryst. Liq. Cryst.*, **2004**, *421*, 197–207.
55. A.S. Desyatnikov, A.A. Sukhorukov and Y.S. Kivshar, "Azimuthons: spatially modulated vortex solitons," *Phys. Rev. Lett.*, **2005**, *95*, 203904.
56. Y.V. Kartashov, L. Torner, V.A. Vysloukh and D. Mihalache, "Multipole vector solitons in nonlocal nonlinear media," *Opt. Lett.*, **2006**, *31*, 1483–1485.
57. B.D. Skuse and N.F. Smyth, "Two-colour vector soliton interactions in nematic liquid crystals in the local response regime," *Phys. Rev. A*, **2008**, *77*, 013817.
58. W. Hu, T. Zhang, Q. Guo, L. Xuan and S. Lan, "Nonlocality-controlled interactions of spatial solitons in nematic liquid crystals," *Appl. Phys. Lett.*, **2006**, *89*, 071111.
59. L.G. Cao, Y.J. Zheng, W. Hu, P.B. Yang and Q. Guo, "Long-range interactions between nematicons," *Chin. Phys. Lett.*, **2009**, *26*, 064209.
60. Y. Izdebskaya, V. Shvedov, A.S. Desyatnikov, Y.S. Kivshar, W. Krolikowski and G. Assanto, " Incoherent interaction of nematicons in bias-free liquid crystal cells," *J. Eur. Opt. Soc.*, **2008**, *5*, 10008.
61. W. Hu, S. Ouyang, P. Yang, Q. Guo and S. Lan, "Short-range interactions between strongly nonlocal spatial solitons," *Phys. Rev. A*, **2008**, *77*, 033842.
62. A.A. Minzoni, N.F. Smyth and A.L. Worthy, "Modulation solutions for nematicon propagation in non-local liquid crystals," *J. Opt. Soc. Amer. B*, **2007**, *24*, 1549–1556.
63. N.F. Smyth and B. Tope, "Beam on beam control: beyond the particle approximation," *J. Nonl. Opt. Phys. Mat.*, **2016**, *25*, 1650046.
64. A. Fratalocchi, A. Piccardi, M. Peccianti and G. Assanto, "Nonlinear management of the angular momentum of soliton clusters: theory and experiments," *Phys. Rev. A*, **2007**, *75*, 063835.
65. S. Skupin, M. Grech and W. Krolikowski, "Rotating soliton solutions in nonlocal nonlinear media," *Opt. Express*, **2008**, *16*, 9118–9131.
66. G. Assanto, N.F. Smyth and A.L. Worthy, "Two colour, nonlocal vector solitary waves with angular momentum in nematic liquid crystals," *Phys. Rev. A*, **2008**, *78*, 013832.
67. A.A. Minzoni and N.F. Smyth, "Theoretical Approaches to Nonlinear Wave Evolution in Higher Dimensions," *Nematicons: Spatial Optical Solitons in Nematic Liquid Crystals*, ed. G. Assanto, John Wiley and Sons, **2012**.
68. M. Shen, X. Chen, J. Shi, Q. Wang and W. Krolikowski, "Incoherently coupled vector dipole soliton pairs in nonlocal media," *Opt. Commun.*, **2009**, *282*, 4805–4809.
69. M. Shen, Q. Kong, J. Shi and Q. Wang, "Incoherently coupled two-color Manakov vector solitons in nonlocal media," *Phys. Rev. A*, **2008**, *77*, 015811.
70. X.H. Wang, Q. Wang, J.R. Yang and J.J. Mao, "Scalar and vector Hermite–Gaussian soliton in strong nonlocal media with exponential-decay response," *Opt. Commun.*, **2017**, *402*, 20–25.
71. S. Lopez-Aguayo, A.S. Desyatnikov, Y.S. Kivshar, S. Skupin, W. Krolikowski and O. Bang, "Stable rotating dipole solitons in nonlocal optical media," *Opt. Lett.*, **2006**, *31*, 1100–1102.
72. S. Zeng, M. Chen, T. Zhang, W. Hu, Q. Guo and D. Lu, "Analytical modeling of soliton interactions in a nonlocal nonlinear medium analogous to gravitational force," *Phys. Rev. A*, **2018**, *97*, 013817.
73. C. Rotschild, O. Cohen, O. Manela and M. Segev, "Solitons in nonlinear media with an infinite range of nonlocality: first observation of coherent elliptic solitons and of vortex-ring solitons," *Phys. Rev. Lett.*, **2005**, *95*, 213904.
74. A. Alberucci, A. Piccardi, R. Barboza, O. Buchnev, M. Kaczmarek and G. Assanto, "Interactions of accessible solitons with interfaces in anisotropic media: the case of uniaxial nematic liquid crystals," *New J. Phys.*, **2013**, *15*, 043011.
75. G. Assanto, N.F. Smyth and W. Xia, "Modulation analysis of nonlinear beam refraction at an interface in liquid crystals," *Phys. Rev. A*, **2011**, *84*, 033818.
76. F. Goos and H. Hänchen, "Ein neuer und fundamentaler Versuch zur Totalreflexion," *Ann. Phys.*, **1947**, *436*, 333–346.
77. G. Assanto, N.F. Smyth and W. Xia, "Refraction of nonlinear light beams in nematic liquid crystals," *J. Nonl. Opt. Phys. Mat.*, **2012**, *21*, 1250033.
78. A.B. Aceves, J.V. Moloney and A.C. Newell, "Theory of light-beam propagation at nonlinear interfaces: I. Equivalent-particle theory for a single interface," *Phys. Rev. A*, **1989**, *39*, 1809–1827.
79. R. Barboza, U. Bortolozzo, G. Assanto, E. Vidal-Henriquez, M. G. Clerc, and S. Residori, "Vortex induction via anisotropy self-stabilized light-matter interaction," *Phys. Rev. Lett.*, **2012**, *109*, 143901.

80. N.F. Smyth and W. Xia, "Refraction and instability of optical vortices at an interface in a liquid crystal," *J. Phys. B: Atomic, Molec. Opt. Phys.*, **2012**, *45*, 165403.
81. A.I. Yakimenko, Yu. Zaliznyak and Yu.S. Kivshar, "Stable vortex solitons in nonlocal self-focusing nonlinear media," *Phys. Rev. E*, **2005**, *71*, 065603.
82. Y.V. Izdebskaya, V.G. Shvedov, P.S. Jung, and W. Krolikowski, "Stable vortex soliton in nonlocal media with orientational nonlinearity," *Opt. Lett.*, **2018**, *43*, 66–69.
83. U.A. Laudyn, M. Kwasny, M.A. Karpierz and G. Assanto, "Vortex nematicons in planar cells," *Opt. Express*, **2020**, *28*, 8282–8290.
84. M. Kwasny, M. A. Karpierz, G. Assanto and U. A. Laudyn, "Optothermal vortex solitons in liquid crystals," *Opt. Lett.*, **2020**, *45*, 2451–2454.
85. G. Assanto and N.F. Smyth, "Soliton aided propagation and routing of vortex beams in nonlocal media," *J. Lasers, Opt. & Photon.*, **2014**, **1**, 1000105: 105–114.
86. H. Zhang, Z. Weng and J. Yuan, "Vector vortex breathers in thermal nonlocal media," *Opt. Comm.*, **2021**, *492*, 126978.
87. H. Zhang, Z. Weng and J. Yuan, "Stabilization of vector vortex beams in thermal nonlinear media," *Optik*, **2021**, *238*, 166686.
88. H. Zhang, T. Zhou and C. Dai, "Stabilization of higher-order vortex solitons by means of nonlocal nonlinearity," *Phys. Rev. A*, **2022**, *105*, 013520.
89. A. Pasquazi, A. Alberucci, M. Peccianti and G. Assanto, "Signal processing by opto-optical interactions between self-localized and free propagating beams in liquid crystals," *Appl. Phys. Lett.*, **2005**, *87*, 261104.
90. Y.V. Izdebskaya, A.S. Desyatnikov, G. Assanto and Y.S. Kivshar, "Deflection of nematicons through interaction with dielectric particles," *J. Opt. Soc. Am. B*, **2013**, *30*, 1432–1437.
91. A. Alberucci, A. Piccardi, U. Bortolozzo, S. Residori and G. Assanto, "Nematicon all-optical control in liquid crystal light valves," *Opt. Lett.*, **2010**, *35*, 390–392.
92. A. Piccardi, M. Peccianti, G. Assanto, A. Dyadyusha and M. Kaczmarek, "Voltage-driven in-plane steering of nematicons," *Appl. Phys. Lett.*, **2009**, *94*, 091106.
93. Y.V. Izdebskaya, "Routing of spatial solitons by interaction with rod microelectrodes," *Opt. Lett.*, **2014**, *39*, 1681–1684.
94. F. Derrien, J.F. Henninot, M. Warenghem and G. Abbate, "A thermal (2D+1) spatial optical soliton in a dye doped liquid crystal," *J. Opt. A: Pure Appl. Opt.*, **2000**, *2*, 332-–337.
95. F. Simoni, L. Lucchetti, D. Lucchetta and O. Francescangeli, "On the origin of the huge nonlinear response of dye-doped liquid crystals," *Opt. Express*, **2001**, *9*, 85–90.
96. L. Lucchetti, M. Gentili and F. Simoni, "Colossal optical nonlinearity induced by a low frequency external electric fields in dye-doped liquid crystals," *Opt. Express*, **2006**, *14*, 2236–2241.
97. A. Piccardi, A. Alberucci and G. Assanto, "Self-turning self-confined light beams in guest-host media," *Phys. Rev. Lett.*, **2010**, *104*, 213904.
98. J.F. Blach, J.F. Henninot, M. Petit, A. Daoudi and M. Warenghem, "Observation of spatial optical solitons launched in biased and bias-free polymer-stabilized nematics," *J. Opt. Soc. Am. B*, **2007**, *24*, 1122–1129.
99. N. Karimi, M. Virkki, A. Alberucci, O. Buchnev, M. Kauranen, A. Priimagi and G. Assanto, "Molding optical waveguides with nematicons," *Adv. Opt. Mater. Commun.*, **2017**, *5*, 1700199.
100. Y.V. Izdebskaya, V.G. Shvedov, G. Assanto and W. Krolikowski, "Magnetic routing of light-induced waveguides," *Nat. Comm.*, **2017**, *8*, 14452.
101. V.G. Shvedov, Y.V. Izdebskaya, Y. Sheng and W. Krolikowski, "Magnetically controlled negative refraction of solitons in liquid crystals," *Appl. Phys. Lett.*, **2017**, *110*, 091107.
102. S. Perumbilavil, M. Kauranen and G. Assanto, "Magnetic steering of beam-confined random laser in liquid crystals," *Appl. Phys. Lett.*, **2018**, *110*, 121107.
103. M. Kwaśny, U.A. Laudyn, K.A. Rutkowska and M.A. Karpierz, "Nematicons routing through two types of disclination lines in chiral nematic liquid crystals," *J. Nonl. Opt. Phys. Mat.*, **2014**, *23*, 1450042.
104. A. J. Hess, G. Poy, J.-S. B.Tai, S. Zumer, and I.I. Smalyukh, "Control of light by topological solitons in soft chiral birefringent media," *Phys. Rev. X*, **2020**, *10*, 031042.
105. A. Piccardi, A. Alberucci, U. Bortolozzo, S. Residori and G. Assanto, "Readdressable interconnects with spatial soliton waveguides in liquid crystal light valves," *IEEE Photon. Techn. Lett.*, **2010**, *22*, 694–696.
106. A. Alberucci, G. Assanto, A.A. Minzoni and N.F. Smyth, "Scattering of reorientational optical solitary waves at dielectric perturbations," *Phys. Rev. A*, **2012**, *85*, 013804.
107. U.A. Laudyn, M. Kwaśny, F.A. Sala, M.A. Karpierz, N.F. Smyth and G. Assanto, "Curved optical solitons subject to transverse acceleration in reorientational soft matter," *Nat. Sci. Rep.*, **2017**, *7*, 12385.
108. F.A. Sala, N.F. Smyth, U.A. Laudyn, M.A. Karpierz, A.A. Minzoni and G. Assanto, "Bending reorientational solitons with modulated alignment," *J. Opt. Soc. Amer. B*, **2017**, *34*, 2459–2466.
109. U.A. Laudyn, M. Kwaśny, M. Karpierz, N.F. Smyth, and G. Assanto, "Accelerated optical solitons in reorientational media with transverse invariance and longitudinally modulated birefringence," *Phys. Rev. A*, **2018**, *98*, 023810.
110. Z. Xu, N.F. Smyth, A.A. Minzoni and Y.S. Kivshar, "Vector vortex solitons in nematic liquid crystals," *Opt. Lett.*, **2009**, *34*, 1414–1416.

111. A.A. Minzoni, N.F. Smyth, A.L. Worthy and Y.S. Kivshar, "Stabilization of vortex solitons in nonlocal nonlinear media," *Phys. Rev. A,* **2009**, *76*, 063803.
112. G. Assanto, A.A. Minzoni and N.F. Smyth, "Deflection of nematicon-vortex vector solitons in liquid crystals," *Phys. Rev. A,* **2014**, *89*, 013827.
113. G. Assanto, A.A. Minzoni and N.F. Smyth, "Vortex confinement and bending with nonlocal solitons," *Opt. Lett.,* **2014**, *39*, 509–512.
114. M.A. Karpierz, M. Sierakowski, M. Swillo and T. Wolinski, "Self focusing in liquid crystalline waveguides," *Mol. Cryst. Liq. Cryst.,* **1998**, *320*, 157–163.
115. M.A. Karpierz, "Solitary waves in liquid crystalline waveguides," *Phys. Rev. E,* **2002**, *66*, 036603.
116. G. Assanto and N.F. Smyth, "Spin-optical solitons in liquid crystals," *Phys. Rev. A,* **2020**, *102*, 033501 (2020).
117. G. Poy, A.J. Hess, I.I. Smalyukh and S. Zumer, "Chirality-enhanced periodic self-focusing of light in soft birefringent media," *Phys. Rev. Lett.,* **2020**, *125*, 077801.
118. M. Warenghem, J.F. Blach and J.F. Henninot, "Thermo-nematicon: an unnatural coexistence of solitons in liquid crystals?," *J. Opt. Soc. Am. B,* **2008**, *25*, 1882–1887.
119. U.A. Laudyn, M. Kwasny, A. Piccardi, M.A. Karpierz, R. Dabrowski, O. Chojnowska, A. Alberucci and G. Assanto, "Nonlinear competition in nematicon propagation," *Opt. Lett.,* **2015**, *40*, 5235–5238.
120. U.A. Laudyn, A. Piccardi, M. Kwasny, M.A. Karpierz and G. Assanto, "Thermo-optic soliton routing in nematic liquid crystals," *Opt. Lett.,* **2018**, *43*, 2296–2299.
121. K. Cyprych, P.S. Jung, Y. Izdebskaya, V. Shvedov, D.N. Christodouliles and W. Krolikowski, "Anomalous interaction of spatial solitons in nematic liquid crystals," *Opt. Lett.,* **2019**, *44*, 267–270.
122. A. Alberucci, U.A. Laudyn, A. Piccardi, M. Kwasny, B. Klus, M.A. Karpierz and G. Assanto, "Nonlinear continuous-wave optical propagation in nematic liquid crystals: interplay between reorientational and thermal effects," *Phys. Rev. E,* **2017**, *96*, 012703.
123. P.S. Jung, W. Krolikowski, U.A. Laudyn, M.A. Karpierz and M. Trippenbach, "Semi-analytical approach to supermode spatial solitons formation in nematic liquid crystals," *Opt. Express,* **2017**, *25*, 23893.
124. P.S. Jung, W. Krolikowski, U.A. Laudyn, M. Trippenbach and M.A. Karpierz, "Supermode spatial optical solitons in liquid crystals with competing nonlinearities," *Phys. Rev. A,* **2017**, *95*, 023820.
125. A. Ramaniuk, M. Trippenbach, P.S. Jung, D.N. Christodoulides, W. Krolikowski and G. Assanto, "Scalar and vector supermode solitons owing to competing nonlocal nonlinearities," *Opt. Express,* **2021**, *29*, 8015–8023.
126. G. Assanto, C. Khan and N.F. Smyth, "Multihump thermo-reorientational solitary waves in nematic liquid crystals: Modulation theory solutions," *Phys. Rev. A,* **2021**, *104*, 013526.